Physica A 457 (2016) 492–505

Contents lists available at ScienceDirect

Physica A

journal homepage: www.elsevier.com/locate/physa

Characterization of the structural collapse undergone by an unstable system of ultrasoft particles

Santi Prestipino [a,b,*], Gianpietro Malescio [a]

[a] Università degli Studi di Messina, Dipartimento di Scienze Matematiche ed Informatiche, di Scienze Fisiche e di Scienze della Terra, Contrada Papardo, I-98166 Messina, Italy

[b] CNR-IPCF, Viale F. Stagno d'Alcontres 37, I-98158 Messina, Italy

HIGHLIGHTS

- We look at the statistical behavior of a Ruelle-unstable model fluid.
- We find two regimes separated by a curve C in the temperature–density plane.
- In the weakly-unstable regime the system behaves as a metastable extensive fluid.
- In the strongly-unstable regime the fluid collapses very quickly to a cluster.
- The separatrix C is the remnant of the liquid–liquid spinodal of a stable fluid.

ARTICLE INFO

Article history:
Received 23 February 2016
Received in revised form 30 March 2016
Available online 8 April 2016

Keywords:
Theory and models of liquid structure
Computer simulation of liquid structure
Liquid–vapor transitions
Phase separation and segregation in colloidal systems

ABSTRACT

The effective repulsion between macromolecules such as polymer chains or dendrimers is everywhere finite, implying that interaction centers can even coincide. If, in addition, the large-distance attraction is sufficiently strong, then the system is driven unstable. An unstable system lacks a conventional thermodynamics since, in the infinite-size limit, it eventually collapses to a finite-size cluster (for instance, a polymer dispersion undergoes irreversible coagulation when increasing the amount of dissolved salt beyond a certain limit). Using a double-Gaussian (DG) potential for demonstration, we study the phase behavior of a system of ultrasoft particles as a function of the attraction strength η. Above a critical threshold η_c, the DG system is unstable but its collective behavior is far from trivial since two separate regions of the thermodynamic plane can be identified, based on the value taken by the average waiting time for collapse: this is finite and small on one side of the boundary, while presumably infinite in the other region. In order to make sense of this evidence, we consider a stable system of particles interacting through a DG potential augmented with a hard core (stabilized DG, or SDG potential). We provide arguments supporting the view that the boundary line of the unstable DG model is the remnant of the spinodal line of a fluid–fluid phase transition occurring in the SDG model when the hard-core diameter is sent to zero.

* Corresponding author at: Università degli Studi di Messina, Dipartimento di Scienze Matematiche ed Informatiche, di Scienze Fisiche e di Scienze della Terra, Contrada Papardo, I-98166 Messina, Italy.
E-mail addresses: sprestipino@unime.it (S. Prestipino), malescio@unime.it (G. Malescio).

http://dx.doi.org/10.1016/j.physa.2016.03.116
0378-4371/

1. Introduction

At variance with atomic fluids, where the interparticle forces are harshly repulsive at short distances due to quantum exclusion, in a number of complex macromolecular fluids the process of integrating out the internal degrees of freedom of each molecule may result in a *bounded* effective repulsion between the centers of mass, thus allowing for full overlap of the interaction centers. For example, dendrimers in a good solvent form highly penetrable coils and the repulsion between the coils, when averaged over molecular conformations, is finite for all distances and decays fast beyond the polymer radius [1]. This effective repulsion may reasonably be represented by a Gaussian function whose width is of the order of the polymer radius and its maximum is a few k_BT [2,3]. In practice, this short-range repulsion is accompanied by an attractive interaction at larger distances, arising from dispersion forces or depletion mechanisms.

The strength of the interpolymer attraction can be tuned by acting on, *e.g.*, the salinity of the dispersion. A sufficiently strong attraction will destabilize the system, causing the polymers to form a dense aggregate, for the finite repulsion would no longer be able to discourage the gathering of the particles all together. This possibility is reflected, even though in more abstract terms, in the known characteristics of pair potentials which are finite at the origin and attractive at large distances. Depending on the attraction strength, a potential of this sort may fall into the category of catastrophic potentials [4], which define systems devoid of a thermodynamic limit. For a stable interaction, the grand-canonical partition function cannot grow faster than $\exp(V/\Lambda^3)$, where V is the system volume and Λ the thermal wavelength. On the contrary, when stability is violated the grand partition function is infinite even for finite V and the system will eventually collapse to a finite cluster. Ruelle [4], and Fisher and Ruelle [5] derived analytic criteria for deciding whether or not a bounded pair repulsion supplemented with a longer-ranged attraction leads to collapse of the system to a non-extensive blob (see next section). However, Ruelle's approach is based on abstract analytic arguments and gives no specific information on the modifications undergone by the phase behavior of the particles as the threshold of thermodynamic stability is approached or even surpassed. Investigating such changes in depth is the aim of the present study. We remark that a process bearing some resemblance to collapse, namely denaturation of dissolved proteins, with the subsequent exposure of hydrophobic groups leading in turn to the formation of insoluble fibrils or other aggregates, is at the heart of important human diseases such as a number of neurodegenerative disorders [6].

To be specific, we inquire into the behavior of particles interacting via a Gaussian pair repulsion at short distances augmented with a weaker shifted-Gaussian attraction at larger distances. Two versions of this so-called double-Gaussian (DG) model, relative to values of the attraction strength far away from the stability threshold, were recently investigated (see Refs. [7,8]). A preliminary account of the behavior of the DG system as a function of the attraction strength, all the way to the stability threshold and also beyond, was given in Ref. [9]. In that paper we reported numerical-simulation evidence that in the unstable regime of the DG model the characteristic time of collapse is enormously different on the two sides of a boundary line. While the decay of an initially homogeneous fluid is very fast in one region (that is, on the high density/low temperature side of the boundary), collapse typically takes a long time to occur in the other region, indeed so long that in a simulation of ordinary length the system is seemingly stable. In the present paper, we concentrate on the nature of the crossover between the two regimes. To this aim, we introduce an interaction potential, now fully stable, obtained from the DG potential through the addition of a hard core of diameter δ. By considering smaller and smaller δ values, we link the behavior of the stabilized DG system to that of the original system, thus finally uncovering the origin and significance of the DG boundary line.

The outline of the paper is as follows. After introducing the DG model in Section 2, we describe our methods in Section 3. Section 4 is devoted to a discussion of the system properties in the unstable regime. In Section 5 we provide a rationale for the existence of a weakly- and a strongly-unstable regime in the DG model, after which we draw our conclusions in Section 6.

2. Model

We study a model of classical point particles interacting through a pair potential taken to be the sum of two Gaussians:

$$u(r) = \epsilon \exp\left\{-\left(\frac{r}{\sigma}\right)^2\right\} - \eta \exp\left\{-\left(\frac{r}{\sigma} - 3\right)^2\right\}, \tag{2.1}$$

where $\epsilon > 0$ and σ are arbitrary energy and length scales (in the following, all energies and lengths are reported in units of ϵ and σ, respectively; see Fig. 1). In Eq. (2.1), the first term is repulsive and is centered at $r = 0$ whereas the second term is attractive ($\eta > 0$) and centered at $r = 3$. Below, we refer to this model as the *double-Gaussian* (DG) model (the $\eta = 0$ case is the *Gaussian-core model* (GCM), a prototype of bounded repulsive interaction [10–13]). Our goal is to study the phase behavior of the DG model as a function of the attraction strength η.

As mentioned in the Introduction, a problem of thermodynamic stability may arise for a system of particles interacting through a repulsive potential which is finite at the origin and attractive at large distances. If the attraction is too strong, a thermodynamic catastrophe occurs in that all particles eventually gather in a finite region of space and the system ceases to be extensive [4,5]. In order to establish whether or not this is the case for the given potential, we resort to a pair of criteria originally put forward by Ruelle (Propositions 3.2.4 and 3.2.7 of Ref. [4]), and recently revived by Heyes and Rickayzen

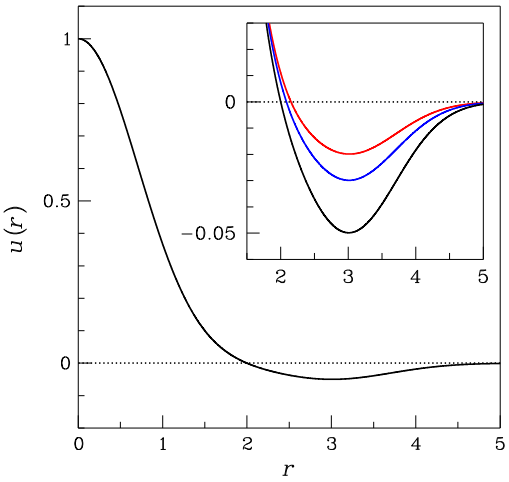

Fig. 1. DG potential for $\eta = 0.05$. In the inset, a comparison is made with the potentials for $\eta = 0.02$ (red) and $\eta = 0.03$ (blue). (For interpretation of the references to color in this figure legend, the reader is referred to the web version of this article.)

(Theorems 1 and 2 of Ref. [14]). Denoting $\widetilde{u}(k)$ the Fourier transform of the potential, a sufficient condition for instability is $\widetilde{u}(0) < 0$. Conversely, if we are able to show that $\widetilde{u}(k) \geq 0$ for all k, then the system is stable.

For the potential in Eq. (2.1), we find $\widetilde{u}(0) < 0$ for $\eta > \eta_c \equiv 0.0263157908\ldots$; below η_c, $\widetilde{u}(k)$ turns out to be positive definite. Hence the DG potential is stable for $\eta < \eta_c$ and unstable for $\eta > \eta_c$ (*i.e.*, an attraction strength of 3% of the repulsion is sufficient to destabilize the system). This apparently implies that it is only meaningful to study the DG system for very minute attractions, while the unstable regime is devoid of any interest. In fact, we shall see that the thermodynamic space of an *unstable* DG fluid is made of two distinct regions separated by a sharp boundary: (a) a region of fully developed instability, where a system prepared in a fluid configuration is going to collapse in very short times; (b) and a "metastable" region, where the waiting time for collapse may be so long that the system is, to all practical effects, stable and extensive. Fantoni and coworkers have observed a similar difference of time scales in the collapse of the unstable penetrable-square-well model [15,16], but no systematic analysis was conducted in that case.

3. Method

3.1. Simulation techniques

In order to reconstruct the statistical behavior of the system, we employed a number of numerical techniques, including molecular dynamics (MD) and a few Monte Carlo (MC) methods. While there is no specific prohibition against using MD to simulate particles interacting through a catastrophic potential, a word is in order for MC simulation. The latter method allows to sample the (Boltzmann's) stationary distribution, which is clearly meaningful only provided that a proper equilibrium is established. Therefore, for a formally unstable system it will have to be carefully checked whether a "temporal" window exists in which the MC averages of macroscopic variables are well defined and take the same values as the MD time averages.

The coexistence between liquid and vapor was mainly probed through Gibbs-ensemble Monte Carlo (GEMC) simulations [17,18]. Even for $\eta > \eta_c$, this method turned out to be a valid tool to study phase coexistence, see Section 4.2. In a GEMC simulation, N particles are initially distributed between two cubic simulation boxes, and arranged in, *e.g.*, a lattice configuration with the same number density for both. Periodic boundary conditions are applied for each box separately. A single GEMC cycle consisted of trial moves of three types: (an average of) N particle shifts within a box, one exchange of volume between the boxes, and a few number (20) of particle swaps (the acceptance rule as well as the schedule of the moves was designed in such a way that detailed balance is satisfied). Particular care was paid in treating the case where one of the box happened to be empty. At very low temperature, in order to achieve a faster equilibration, we found useful to start with largely different numbers of particles in the two boxes (in this case, we write $N_1 + N_2$ to indicate that we initially put N_1 particles in one box and N_2 particles in the other). Typically, 4×10^5 GEMC cycles were enough for equilibrium quantities, with averages computed over the second half of the trajectory only.

Far from coexistence, the nature of the system equilibrium for $\eta > \eta_c$ was investigated by standard *NVT* (*i.e.*, canonical-ensemble) Metropolis MC with periodic boundary conditions. The important quantity to look at is the total system energy E: an average energy proportional to N is the hallmark of (meta)stable equilibrium, whereas an energy value scaling faster than N, typically as N^2, is the imprint of system collapse. Anticipating the main result from the next section, a *NVT* simulation of an unstable fluid either leads to the quick collapse of the system to a small blob, or proceeds for long time as if the fluid were fully stable (in this case, we found no appreciable size dependence of the thermal averages).

We employed MD simulations both to check that the outcome of the MC runs is consistent with the natural system dynamics even in the unstable region, and to evaluate the characteristic time for collapse as a function of the system density for a fixed temperature. Temperature control was implemented through a velocity-Verlet algorithm combined with rescaling of particle velocities at the previous time step (in the long run, the time-averaged kinetic energy becomes consistent with the temperature set in the program input).

3.2. Integral equations

Despite its many advantages, numerical simulation faces two limitations. First, simulation is impractical for extensive investigations of the behavior of several thousand particles due to relevant cpu-time requirements. Second, since the number of simulated particles is necessarily finite, the importance of finite-size effects must be checked with care.

Distribution-function theories [19] (*viz.*, integral equations of liquids) represent an alternative approach which does not suffer from these shortcomings. Since an integral equation describes the system as homogeneous, in the region of thermodynamic plane where the equation admits no solution the system does not exist as a homogeneous fluid, at least within the accuracy of the equation considered. Hence, integral equations can be employed to draw the boundary line (BL) separating the region of thermodynamic parameters where the equation can be solved ("stable" region) from the ("unstable") region where no homogeneous-fluid solution exists. Upon approaching the BL from the stable region, the computed isothermal compressibility usually attains increasingly large positive values (though it does not generally diverge on the BL).

For simple-fluid potentials, featuring an unbounded short-range repulsion and an attractive tail, the BL can be put in correspondence with the liquid–vapor *spinodal* line. In general, the spinodal line marks the threshold of homogeneous-system stability against phase separation. Within this curve, even infinitesimally small density fluctuations immediately lead to phase separation via a process called *spinodal decomposition*. Outside the spinodal line, the homogeneous fluid is stable, or at least metastable with respect to density fluctuations. The spinodal line lies inside the *binodal* (coexistence) curve, which is defined by the requirement that the temperature, pressure, and chemical potential be the same for both liquid and vapor phases. The region enclosed between the binodal and the spinodal curve is a region of metastable equilibrium where the system can exist as a single phase only for a finite period of time.

A well-known deficiency of integral equations is the lack of thermodynamic consistency (*i.e.*, different thermodynamic routes yield different equations of state for the fluid). Many recipes have been proposed in order to produce thermodynamically-consistent integral equations, which usually lead to more accurate estimates of structural and thermodynamic properties at the expenses of more cumbersome solution procedures. The accuracy of a number of integral equations, including the simple hypernetted-chain (HNC) equation [19] and two thermodynamically-consistent approaches, namely the Rogers–Young closure [20] and the zero-separation closure [21], was investigated for the GCM [22] (the Percus–Yevick closure [19], which is quite accurate for the steeply-repulsive potentials, is not suited for the GCM). When compared to simulation results, the HNC theory underestimates the system structure for small to moderate packings; however, it is extremely accurate for high densities where the GCM fluid only weakly departs from the structure of an ideal gas. Moreover, the HNC equation is not affected by a recurrent problem of self-consistent closures, that is the existence of spurious solutions.

Recently, an investigation of the stable and unstable regions of the HNC equation was performed for the penetrable-square-well model, consisting of penetrable spheres subjected to a square-well attraction outside the core [23]. Compared to numerical simulations [15,16], the HNC equation yielded reasonable indications on the phase behavior with much less computational effort. For the purpose of the present investigation, the HNC equation is then preferable to more sophisticated (but harder to manage) closures. The accuracy of the HNC equation for ultrasoft particles was investigated at lengths by Likos et al. in Refs. [24,25], where it was shown that mean-field density functional theory becomes exact at high temperatures and/or densities. We hereafter present an argument, based on the assumption of ideal-gas structure of the DG system at high density, which aims to determine the behavior of the BL in the unstable regime.

On general grounds, the isothermal compressibility K_T is related to the integral of the total correlation function $h(r)$ all over space, through the formula:

$$\rho k_B T K_T = 1 + \rho\widetilde{h}(0) = \frac{1}{1 - \rho\widetilde{c}(0)}, \tag{3.1}$$

where ρ is the number density and $c(r)$ is the direct correlation function. In light of the conclusions of Refs. [22,24,25], for all bounded potentials having a Gaussian core we admit that

$$h(r) \approx 0 \quad \text{for } \rho > \rho_0(T), \tag{3.2}$$

$\rho_0(T)$ being a characteristic system density expected to be higher the lower T is. Within the above assumption, for $\rho > \rho_0$ the HNC expression of $c(r)$ reads:

$$c(r) = h(r) - \ln[1 + h(r)] - \beta u(r) \approx -\beta u(r), \tag{3.3}$$

saying that, for high enough densities, the HNC theory reduces to the *random-phase approximation* (RPA), and therefore $K_T^{(\mathrm{HNC})} \approx K_T^{(\mathrm{RPA})}$ or

$$\rho k_B T K_T^{(\mathrm{HNC})} \approx \frac{1}{1+\rho\beta\widetilde{u}(0)}. \tag{3.4}$$

If $\widetilde{u}(0) > 0$ (which for the DG potential is synonymous of stability) then $K_T^{(\mathrm{HNC})}$ is small and positive for sufficiently high ρ, implying that the BL cannot extend to infinite ρ. Conversely, if $\widetilde{u}(0) < 0$ (*i.e.*, the DG potential is Ruelle-unstable) then $1/K_T^{(\mathrm{HNC})}$ changes sign continuously at a certain T-dependent density, meaning that (at least, within the approximate (3.4) formula) $K_T^{(\mathrm{HNC})}$ diverges at the BL, which in turn is located at

$$\rho\beta\widetilde{u}(0) = -1 \Longrightarrow k_B T = |\widetilde{u}(0)|\rho. \tag{3.5}$$

For $k_B T > |\widetilde{u}(0)|\rho$, the HNC value of K_T is strictly positive and the homogeneous fluid is thoroughly stable. Eq. (3.5) is a well-definite prediction of assumption (3.2), which we shall check below for the DG model against the numerically-computed BL.

4. Results

4.1. The stable regime

We briefly report on the phase behavior of the DG model for attraction strengths smaller than the thermodynamic-stability threshold η_c [9].

Far below η_c, the DG model exhibits a conventional liquid–vapor transition at low ρ and T, with a bell-shaped coexistence line [7,8]. As the attraction gets stronger, the coexistence region increases in extent until, close to the stability threshold, the binodal line undergoes a remarkable modification at low T, where it substantially widens. For the same temperatures, the density ρ_l of the saturated liquid acquires a strong dependence on the system size (see Fig. 1 in Ref. [9]). An analogous trend as a function of η is observed in the BL of the HNC theory, which at low temperature also widens, apparently without bounds in the combined $\eta \to \eta_c$ and $T \to 0$ limits (inset of Fig. 1 in Ref. [9]).

As far as the solid phase is concerned, for very high densities it would only be stable for exceptionally low temperatures. Indeed, according to the melting criterion formulated in Ref. [26], the DG melting temperature would reach a maximum of $T_M \approx 0.01$ for a density $\rho_M \approx 0.22$ (the height and abscissa of the maximum are nearly insensitive to η), beyond which it rapidly decays with increasing density.

4.2. The unstable regime

In the unstable regime no thermodynamic limit exists. Keeping this in mind, we investigated the behavior of the DG system with care, by first employing the HNC equation. The results of this analysis are later used as a broad guide to a more accurate study of the model in terms of numerical simulation.

For attraction strengths larger than η_c, the BL of the HNC theory again divides the ρ–T plane in two regions (see Fig. 2). Above the BL, the iterative procedure to solve the HNC equation leads to convergence and the system can be described as a homogeneous fluid. However, since the HNC theory is thermodynamically inconsistent, and thus blind to the system instability, this fluid can at best be *metastable*. In the region below the BL, which for $\eta > \eta_c$ is of infinite extent, no solution to the HNC equation is found and the homogeneous fluid is then unstable. Hence, according to the HNC theory, above the stability threshold the DG system would be mechanically unstable for each temperature T *but* only beyond a T-dependent density.

In the narrow interval $\eta_c < \eta < \bar{\eta} \simeq 0.0270$, the BL exhibits a local maximum for $\rho \approx 0.2$, followed by a minimum at a higher density, beyond which the BL asymptotically becomes a straight line. For $\eta = \bar{\eta}$, the maximum and the minimum coalesce and, from there onward, the BL becomes a monotonically increasing function of ρ. As η progressively grows, the BL increasingly resembles a straight line, even for low densities.

These findings are consistent with the following scenario. For $\eta_c < \eta < \bar{\eta}$, the low-density system undergoes a transition from a metastable vapor to a metastable liquid which, as the density is further increased, eventually disappears. As η overcomes $\bar{\eta}$, the distinction between liquid and vapor vanishes and the mechanically-unstable region grows in extension with increasing η.

For every $\eta > \eta_c$, the BL becomes a straight line for very large densities, whose slope increases linearly with η, irrespectively of the BL shape at small density (see Fig. 2 inset). To a very high precision, the asymptotic BL slope coincides with $|\widetilde{u}(0)|$, thus giving credit to the conjecture made in the previous section on the $h(r)$ function (cf. Eqs. (3.2) and (3.5)). Upon extrapolating the linear behavior of the slope down to zero, we can estimate the value η_0 of the attraction strength above which the slope is strictly positive, which is also the value of η separating the stable from the unstable regime. By including in the fit also values of η quite far away from the stability threshold (and up to 0.05) we obtained $\eta_0 = 0.026320$, a number very close to η_c. An even better η_c estimate is obtained if the fit is restricted to a range of values closer to η_c. For

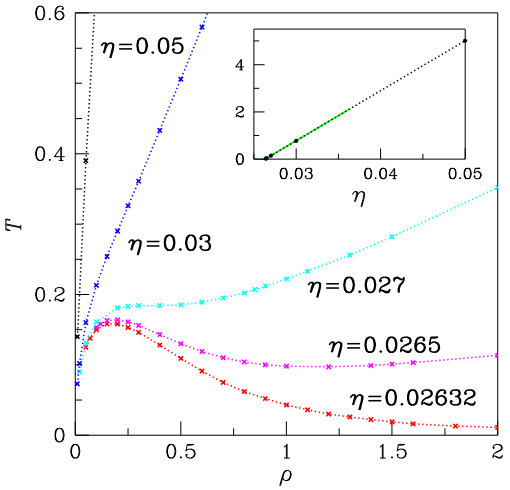

Fig. 2. DG system, BL of the HNC theory for a number of η values above the thermodynamic-stability threshold: 0.02632 (red), 0.0265 (magenta), 0.027 (cyan), 0.03 (blue), and 0.05 (black). Notice that the BL for $\eta = 0.02632$ reaches a local minimum for $\rho \approx 3.8$. Inset: asymptotic BL slope, plotted as a function of η. The black dotted line is the straight line providing the best (least-square) fit of the data in the interval 0.0264–0.05. The green line is $|\widetilde{u}(0)|$ vs. η. (For interpretation of the references to color in this figure legend, the reader is referred to the web version of this article.)

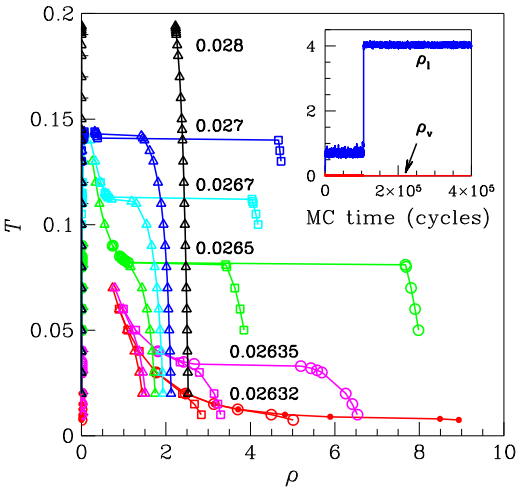

Fig. 3. DG system, liquid–vapor coexistence densities for a number of η values above the thermodynamic-stability threshold: 0.02632 (red), 0.02635 (magenta), 0.0265 (green), 0.0267 (cyan), 0.027 (blue), and 0.028 (black). The various symbols correspond to different N_1 and N_2 values: 864 + 864 (triangles), 4000 + 108 (squares), 8192 + 128 (open dots), and 16 000 + 128 (small full dots). Inset: system density in the two simulation boxes, plotted as a function of simulation time, for $\eta = 0.0267$, $N = 4000 + 108$, and $T = 0.112$—*i.e.*, slightly below $T^*(0.0267)$. (For interpretation of the references to color in this figure legend, the reader is referred to the web version of this article.)

example, only considering the slopes for $\eta = 0.0264$, 0.0265, and 0.027, we got $\eta_0 = 0.026317$. We conclude that the HNC equation allows to extract the stability threshold with great precision from both sides of η_c.

Turning to simulation, we first checked by GEMC the existence of a (metastable) coexistence between liquid and vapor in the range $\eta_c < \eta < \bar{\eta}$. Specifically, we simulated various samples for a number of η values (see Fig. 3). Two distinct cases occurred: either coexistence is quickly established and coexistence densities are roughly insensitive to the sample size, or, when the temperature is low enough, coexistence is still established but the density of the saturated liquid grows almost linearly with N, signaling that the denser phase is actually a non-extensive blob (in this case, the coexistence density of the vapor is nearly zero). For each η the transition between the two cases is very sharp, occurring at a temperature T^* which is higher the larger η is. At the lowest η considered (0.02632, just above the stability threshold), T^* is as low as 0.01 but we needed our largest size (that is, 16 000 + 128) to observe the mentioned crossover.

The above evidence confirms what suggested by the HNC equation. For $\eta_c < \eta < 0.027 \simeq \bar{\eta}$, the liquid–vapor transition only exists above a certain temperature $T^*(\eta)$ (the HNC estimate of T^* is nothing but the relative minimum of the BL). For $\eta = 0.028$, liquid and vapor no longer survive as distinct phases. Near below the crossover temperature $T^*(\eta)$, and provided that N is sufficiently large, we systematically observed a sudden switch from standard liquid–vapor separation (which is the early choice made by the system) to formation of a condensate with a N-dependent density (see Fig. 3 inset).

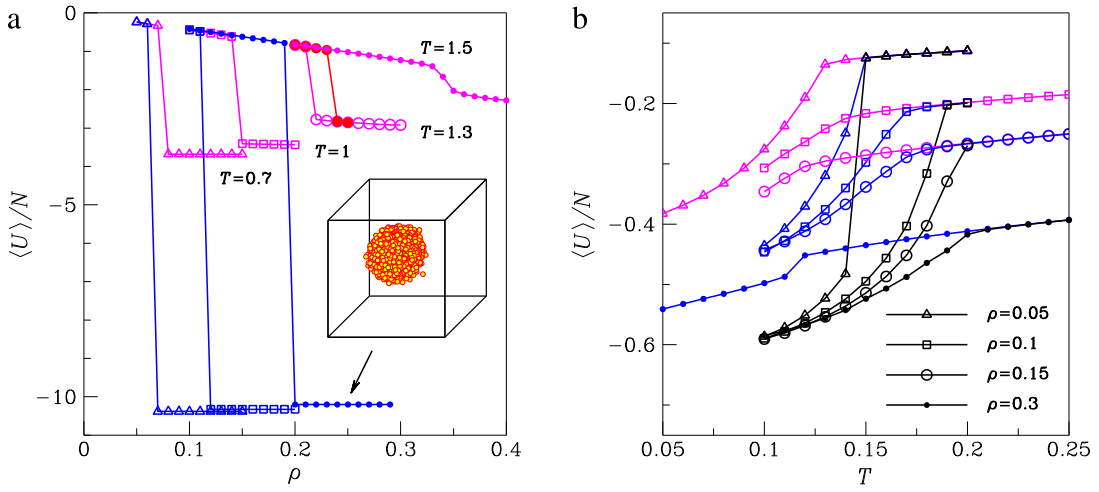

Fig. 4. Unstable DG fluid, average potential energy per particle as a function of density and temperature. (a) $\eta = 0.06$, two sample sizes ($N = 1372$, magenta; and $N = 4000$, blue), and various temperatures ($T = 0.7$, triangles; 1, squares; 1.3, open dots; and 1.5, small full dots). The red full dots mark the outcome of MD simulations carried out in sequence, starting from $\rho = 0.2$, for $N = 1372$ and $T = 1.3$ (each run consisted of 4×10^6 time steps, with the averages computed over the second half of the trajectory only). Inset: snapshot of a typical collapsed configuration of the $N = 4000$ system, taken for $\rho = 0.25$ and $T = 1.5$ (here the box length is 25.20). In preparing this figure, we gave each particle a diameter of σ. (b) $\eta = 0.03$, three sample sizes ($N = 1372$, magenta; $N = 4000$, blue; and $N = 8192$, black), and a few densities ($\rho = 0.05$, triangles; 0.1, squares; 0.15, open dots; and 0.3, full dots). For such a small η, only very large sizes bear traces of collapse in the behavior of the energy. (For interpretation of the references to color in this figure legend, the reader is referred to the web version of this article.)

To better elucidate the nature of the metastable-to-unstable transition and also unveil the structure of the collapsed state, we carried out a series of *NVT* simulations for many different combinations of η, N, and T (in particular, we analyzed the cases $\eta = 0.03$, 0.06, 0.09, and 0.2). A typical set of results is reported in Fig. 4(a), referring to $\eta = 0.06$. We here show potential-energy data for two sizes, $N = 1372$ and $N = 4000$, and four temperatures, $T = 0.7$, 1, 1.3, and 1.5. These data were obtained by performing simulation runs sequentially, starting for a given density from the last system configuration generated at the previous (slightly smaller) density. Each run was 2×10^6 cycles long, with averages computed over the last million cycles only. We see that the average potential energy per particle, which is independent of N at low density, for a certain T-dependent density ρ^* drops abruptly to a large negative value which, in absolute terms, scales as N. Hence, the total energy becomes of the order of N^2, which is the distinctive feature of the formation of a dense, non-extensive blob comprising all particles in the system. As can be appreciated from the inset of Fig. 4(a), which shows an image of the 4000-particle system for $\rho = 0.25$ and $T = 1.5$, the visual appearance of the collapsed system is that of a compact spherical cluster which fills only a part of the simulation box. Clearly, the spherical shape responds to the necessity of minimizing the surface-energy cost. We found that, while still depending on T, the cluster radius is roughly independent of N, meaning that the cluster density increases linearly with N.

Already after collapse, the system energy attains its lowest possible value (*i.e.*, a further compression of the system does not make the energy smaller). Upon increasing N, ρ^* slightly decreases. Moreover, when the sample is small the collapse transition gets rounded (*i.e.*, smeared in density) for high temperatures and/or densities. This is particularly evident for $\eta = 0.03$, see Fig. 4(b), where we observed a distinct energy jump on cooling only for the lowest density considered, $\rho = 0.05$, and for the biggest size employed, $N = 8192$.

In Fig. 5 we collected the (ρ, T) points where system collapse first occurred, under either isothermal compression ($\eta = 0.06, 0.09, 0.2$) or isochoric cooling ($\eta = 0.03$). Each group of lines refers to a specific η value, and there is one line for each value of N (we also plotted the BL of the HNC equation for comparison). We see that the simulation loci assume a definite limiting position as N grows; moreover, there is a striking correspondence between the BL and the simulation data for the highest N. These facts together suggest that, for $\eta > \eta_c$, the extensive-to-nonextensive crossover occurs for a distinguished non-zero density *even in the infinite-size limit*, that is, there is a sharp line separating two distinct dynamic regimes: a "long-lasting metastability" regime, where the time we should typically wait for collapse to manifest enormously exceeds our simulation times (say, a few million MC cycles). In the other regime of "full-fledged instability", collapse occurs fast, well within the length of our runs.

A suggestive interpretation of the above findings is the following. The locus of points $\rho^*(T)$ where a large-sized DG fluid first collapses is a sort of *spinodal* line (well approximated by the HNC BL), separating a metastable vapor region (on the low-density side) from a two-phase region (on the high-density side) where a *vanishing-density vapor* coexists with a *huge-density liquid*. For $\rho < \rho^*(T)$, the vapor is metastable and the system appears homogeneous and extensive. As ρ overcomes ρ^*, the metastable vapor instantly decays to a heterogeneous system consisting of a spherical huge-density liquid cluster in a vanishing-density vapor background. Below $\rho^*(T)$, the liquid cluster should also form, but it will take a rather long time to nucleate, so long that it far exceeds our simulation times.

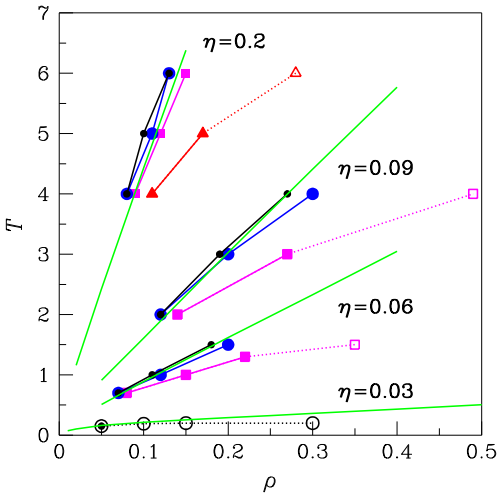

Fig. 5. DG system above the thermodynamic-stability threshold ($\eta = 0.03, 0.06, 0.09, 0.2$). The loci are shown where the crossover from the extensive to the nonextensive behavior first occurred: $N = 500$ (red triangles), 1372 (magenta squares), 4000 (blue dots), and 8788 (8192 for $\eta = 0.03$, black dots). In these MC simulations, ρ was increased in steps of 0.01 at constant T (for $\eta = 0.03$, it is T that was reduced in steps of 0.01 at constant ρ). The density point where a sharp energy drop was observed has been marked by a full symbol, whereas an open symbol represents the approximate location of a more diffuse (in density or in temperature) energy drop. The green lines are the boundary lines of the HNC theory. (For interpretation of the references to color in this figure legend, the reader is referred to the web version of this article.)

To learn more about the position and width of the crossover region between the two regimes, as well as to clarify the stochastic character of the collapse event, we carried out a large number of MD simulations of the DG model (at various densities and sizes, for fixed $\eta = 0.2$ and $T = 6$) where N particles, originally distributed at random in the box, are followed during their evolution (usually for many million MD time steps near the threshold of dynamic crossover) until collapse occurs, *i.e.*, until a sharp drop of the total energy is detected. In these simulations, the time step used was $\Delta t = 10^{-3}$ (in reduced, $\sigma\sqrt{m/\epsilon}$ units, m being the particle mass). As a preliminary task, for a number of η values above η_c we verified that, in the metastable region, canonical-ensemble MC averages (that is, energy and virial pressure) indeed coincide with MD averages. Moreover, with both techniques the dynamic crossover is located at about the same place. Hence, also for MD, the phase-space basin pertaining to the fluid is separated/protected from the absorbing (cluster) states by a large activation barrier; within this basin, the system is fully thermalized. For example, Fig. 4(a) shows some MD energy data for the case $\eta = 0.06$ and $T = 1.3$. Here collapse occurred for a density which is slightly larger than the crossover density signaled by MC (0.24, rather than 0.22), but this would just be a consequence of the activated nature of the collapse event, which makes the time scales of MD and MC non-comparable (see more below).

For a number of densities in the crossover region, we followed the time evolution of the system energy for 10^6 time steps after the initial preparation in a homogeneous-fluid state. As documented in Ref. [9], the energy of $N = 1372$ particles eventually undergoes a sudden drop, rather well resolved in time, corresponding to the onset of collapse. As N grows, however, the nature of collapse gradually changes, since an increasing number of plateaus appear in the energy chart. Such an event is already observed for $N = 2048$ (see Fig. 4 of the Supplemental Material for Ref. [9]), where the only plateau present corresponds to the simultaneous formation of two clusters, both surviving for a small period of time before coalescing in a single cluster. A more spectacular energy evolution is seen in Fig. 6(a), which refers to a 4000-particle system, for fixed $\eta = 0.2$ and $T = 6$ and a few densities in the range 0.145–0.150. We see that the energy evolves through a series of plateaus alternated with sudden drops, each corresponding to a reorganization of particles in space, as illustrated in Fig. 6(b). Here, the initial number of clusters is 5 (a number expected to grow with N), but they subsequently merge upon collision until one cluster only is left at the end. This coarsening phenomenon resembles Ostwald ripening (see e.g. Ref. [27]). Every time two clusters come close to each other, one of them quickly absorbs the particles of the other but, rather than increasing in size at the expenses of the other, the surviving cluster has approximately the same size of its parents (hence the density of the unique cluster left at the end is about 5 times larger than the density of the original clusters).

Now moving to a more systematic analysis, we performed from 31 to 51 independent runs for each investigated density in the extensive-to-nonextensive crossover region. For every run, we took note of the instant when the energy dropped for the first time, which was then averaged over the totality of the runs. In Fig. 7 we plot the mean waiting time for collapse, $\bar{t}$, as a function of density, for three sizes ($N = 864, 1372, 2048$). A distinct $\bar{t}$ increase is seen to occur near the location of the collapse transition signaled by MC. Especially for the lowest densities, the distribution $P(t)$ of waiting times is very dispersed around the mean and also increasingly skewed to the right the smaller the density (as can also be argued from the non coincidence of median and mean). At such low densities, collapse sometimes occurred after such a long span of time that the effort of pushing the analysis to still smaller densities would be too costly. From looking at the data of Fig. 7, it would be hard to say whether, in the infinite-size limit, the *average* waiting time for collapse would blow up to infinity below a

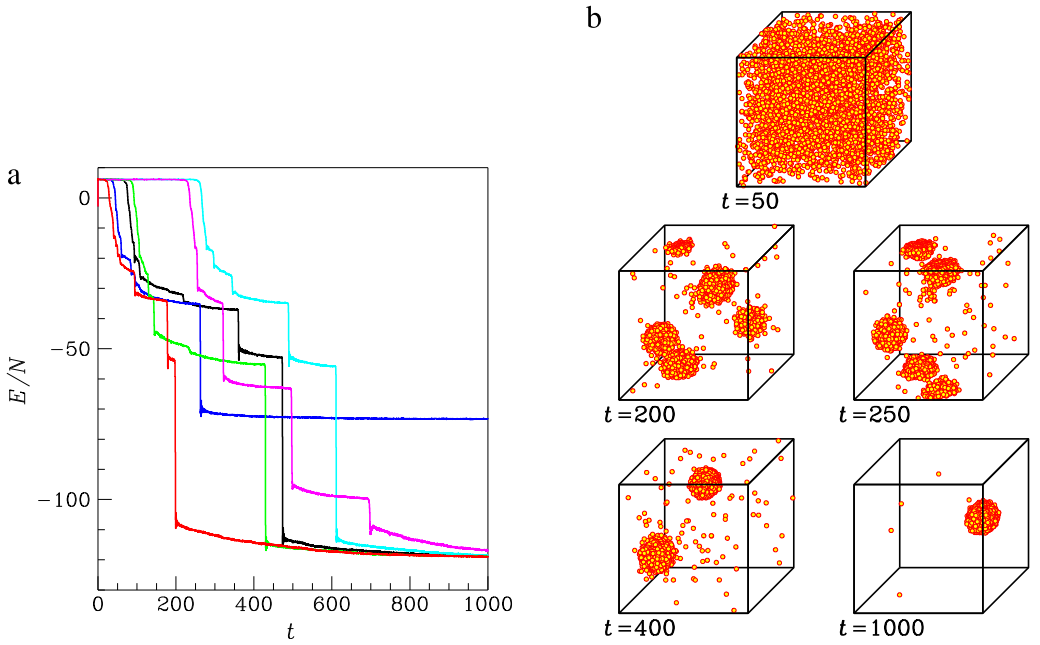

Fig. 6. DG system for $\eta = 0.2$ and $T = 6$. (a) Energy evolution of a $N = 4000$ system during a run of 10^6 MD steps, for six different densities: $\rho = 0.145$ (black), 0.146 (blue), 0.147 (cyan), 0.148 (green), 0.149 (magenta), and 0.150 (red). Successive energy drops correspond to sudden modifications of the overall system conformation. (b) The picture shows five successive configurations of a $N = 4000$ system in the $\rho = 0.145$ run (recall that periodic conditions are applied at the boundary of the box). The homogeneous fluid initially collapses at $t \simeq 90$, through the simultaneous formation of 5 clusters. These became 4 already at $t \simeq 110$. As dynamical evolution goes on, the clusters first reduced to 3 ($t \simeq 215$), then to 2 ($t \simeq 355$), and finally to 1 ($t \simeq 470$). (For interpretation of the references to color in this figure legend, the reader is referred to the web version of this article.)

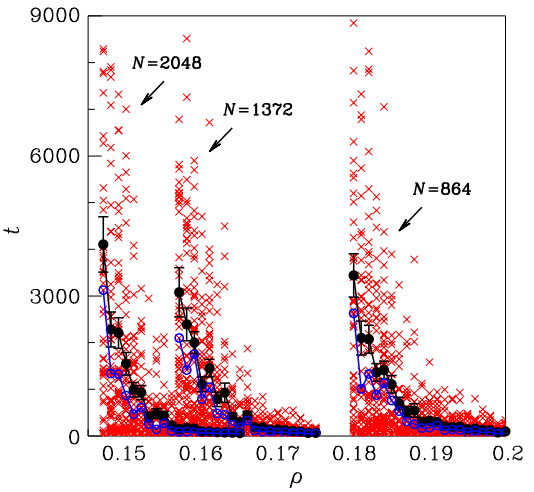

Fig. 7. DG system above the thermodynamic-stability threshold ($\eta = 0.2$ and $T = 6$): collapse times (red crosses) for each of 31 MD runs (51, for the lowest five densities in each group) carried out for a few densities in the ranges 0.147–0.165 ($N = 2048$), 0.157–0.175 ($N = 1372$), and 0.180–0.200 ($N = 864$). Notice that some of the red crosses are not shown since they fall outside the t range considered. The black dots are arithmetic averages over each set of 31 or 51 instances (the error-bar length is twice the standard error of the mean, *i.e.*, twice the unbiased sample standard deviation divided by $\sqrt{31}$ or $\sqrt{51}$). Also shown are the median times (blue open dots).

non-zero density, or rather it will keep on increasing upon reducing ρ further. The former possibility is actually more likely, considering the trend of the data in Fig. 5 with system size and the correspondence existing between the location of the $\bar{t}$ rise for large N and the HNC BL. As a further experiment, we carried out 20 independent MD runs of very long length (4×10^7 time steps), for $N = 864$ and $\rho = 0.150$ (*i.e.*, well inside the metastable region), starting from an always different gaseous configuration: as a matter of fact, for none of these runs collapse occurred within the prescribed time limit.

A possible mechanism for the divergence of $\bar{t}$ at a non-zero crossover density is a probability distribution $P(t)$ of waiting times developing, below a certain density, a fat tail of the kind $t^{-\alpha}$, with $1 < \alpha < 2$ (in this case, $tP(t)$ is not integrable but $P(t)$ is still normalizable). Should this be the truth, collapse will eventually occur at any point of the metastable region,

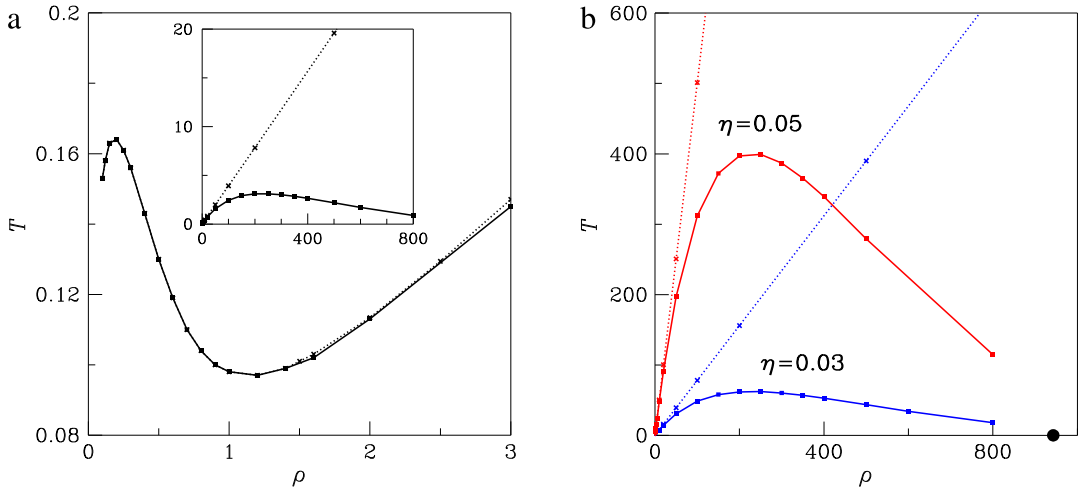

Fig. 8. BL of the HNC theory for the SDG model. (a) Low-density behavior of the BL for $\eta = 0.0265$, for two values of the diameter δ: $\delta = 0$ (DG model, crosses) and $\delta = 0.1$ (full squares). Inset: high-density behavior. (b) High-density behavior of the BL for $\eta = 0.03$ (blue) and $\eta = 0.05$ (red): $\delta = 0$ (crosses) and $\delta = 0.1$ (full squares). The black dot marks the freezing density of hard spheres with diameter δ. (For interpretation of the references to color in this figure legend, the reader is referred to the web version of this article.)

but the time it typically takes for the system to collapse is not bounded from above. In other words, if one waits enough, it will always happen to observe a yet larger value of the variable t. This means that, upon repeating the simulation again and again (starting each time from a different initial configuration), we will always find collapse times larger than any value observed before.

To sum up, in the unstable regime a DG system prepared in a cluster configuration will remain a cluster forever. Indeed, such cluster configurations are *absorbing states* for the system dynamics (be it fictitious or real). However, if the system is prepared in a *homogeneous* (fluid) state, then the time it takes for the system to collapse in a cluster crucially depends on the values of ρ and T (for fixed values of N and η). For sufficiently large N, a well-definite line separates a region of very fast decay to a droplet from another region where relaxation is extremely slow. We conjectured that the probability distribution of collapse times develops a fat tail when the initial fluid density is below the threshold value on the separatrix. This does not exclude that the thermodynamically-unstable system eventually collapses for every density and temperature.

5. The collapse phenomenon as a limiting case of spinodal instability

In order to delve more deeply into the nature of the collapsed state, we consider a system of particles interacting through the (stabilized-DG, *i.e.*, SDG) potential

$$u_{\mathrm{SDG}}(r) = \begin{cases} +\infty, & r < \delta \\ u_{\mathrm{DG}}(r), & r \geq \delta \end{cases} \tag{5.1}$$

(δ is the particle diameter). For δ smaller enough than σ, the system is expected to behave similarly as the DG model, at least up to intermediate densities, deviating from it only for larger densities (*i.e.*, as the inner core becomes effective). The addition of a hard core to the DG potential prevents the collapse of the system, making it *fully thermodynamically stable* (by Corollary B in Ref. [5]).

5.1. HNC theory

We first discuss the evolution of the BL of the HNC theory with δ and η, postponing the analysis of simulation results until below in this Section. In Fig. 8(a), we show the BL for $\delta = 0.1$ and $\eta = 0.0265$. For small densities, the SDG BL is indeed indistinguishable from the BL of the DG model. The stabilizing effect of the core causes the SDG BL to substantially deviate from the DG BL only for higher densities, see Fig. 8(b), where the former line develops a broad maximum (for $\rho \approx 200$ when $\delta = 0.1$, moving down to $\rho \simeq 2$ when $\delta = 0.5$). Upon compression, at some point the BL will cross the melting line since, for sufficiently large densities, the stable phase of the SDG model is a face-centered cubic crystal. The onset of crystallization is expected to occur near the freezing point of hard spheres with diameter δ (*i.e.*, for $\rho\delta^3 \approx 0.943$). Note that the abscissa of the BL maximum also approximately scales as δ^{-3}, indicating that the δ length is already effective for moderate densities.

The above findings can be rationalized as follows. The SDG potential is an example of soft-core potential, where an infinitely-repulsive core is "softened" through the addition of a finite repulsion (in our case, the Gaussian repulsion). Such potentials are characterized by two *repulsive length scales* (see, *e.g.*, Ref. [28]): a smaller "hard" length and a larger "soft" length. These length scales give origin to a more compact and a looser particle arrangement, respectively. The effectiveness

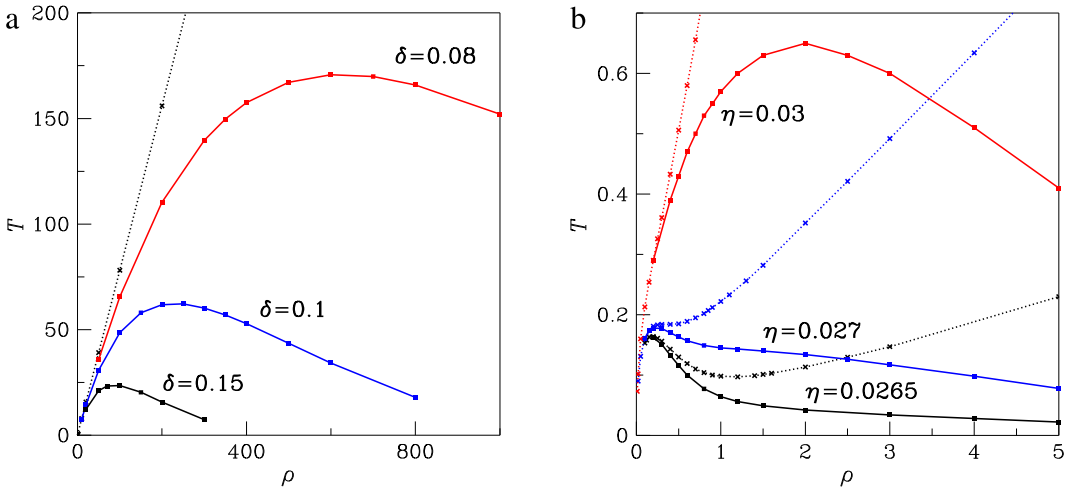

Fig. 9. SDG model, HNC BL plotted as a function of ρ. (a) δ evolution of the BL for $\eta = 0.03$: $\delta = 0$ (DG model, crosses and dotted line), 0.08 (red squares), 0.1 (blue squares), and 0.15 (black squares). (b) η evolution of the BL for $\delta = 0.5$: $\eta = 0.0265$ (black squares), 0.027 (blue squares), and 0.03 (red squares). The dotted lines are for the DG model. (For interpretation of the references to color in this figure legend, the reader is referred to the web version of this article.)

of the two length scales depends on the values of pressure and temperature. The "soft" length is only effective for low pressures and temperatures, whereas the "hard" length becomes important for higher pressures and temperatures. For those pressures and temperatures where the two scales are both effective, we see the competition between a denser and a looser local particle arrangements, and the fluid behaves as if it were a mixture of two particle species with different radii.

When the attractive component of the potential is not too strong, a soft-core potential gives rise to two distinct liquid phases: a low-density liquid (LDL, associated with the soft length) and a high-density liquid (HDL, associated with the hard length). This behavior is mirrored in the shape of the SDG BL, which has two maxima for $\eta_c < \eta < \bar{\eta}$, one related to a LDL–vapor critical point and the other to a HDL–LDL critical point [29]. While the critical density of the LDL–vapor transition is related to the soft length, the critical density of the HDL–LDL transition is related to the hard length. The ratio between the two critical densities is of the order of $(\sigma/\delta)^3$.

We explored the high-density behavior of the BL of the SDG model as a function of the hard-core diameter δ (see Fig. 9(a)), choosing a value of the attraction strength ($\eta = 0.03$) for which the BL has only one maximum (therefore, only a vapor and a HDL phase exist). As δ gets smaller, the BL maximum occurs for higher and higher densities and temperatures; likewise, the range of densities over which the boundary lines of the SDG and DG models are practically indistinguishable extends to higher densities. For $\delta = 0$, the SDG potential becomes identical to the DG potential, and the BL of the latter is recovered. In Fig. 9(b), we follow the evolution of the BL as a function of η for fixed $\delta = 0.5$. We see that, as η diminishes, the broad maximum centered at $\rho \simeq 2$ becomes gradually depressed, until it disappears altogether slightly above η_c. This behavior highlights the gradual vanishing of the liquid–liquid transition as η falls below the critical attraction strength.

Summarizing, the repulsive length of the SDG potential which sets the scale of the HDL structure, bringing to a stop the aggregation cascade driven by the attractive forces, is the hard-sphere diameter δ. As δ gets smaller, the saturated HDL density grows more and more, until it goes to infinity in the $\delta \to 0$ limit. In the same limit, the ascending branch of the HDL–vapor *spinodal* line will match the locus which, in the unstable DG model, separates the extensive from the non-extensive region. Therefore, the cluster forming in an unstable DG fluid of $N \gg 1$ particles can be viewed as the finite-size manifestation of a fluid phase of infinite density. In other words, the onset of collapse is the mark of a "condensation" transition where there is no repulsive core that could prevent particles from crowding all together. Also in common condensation the first occurrence of liquid–vapor separation in a *NVT* setting is the formation of a spherical cluster [30–32]. The main difference with the DG cluster is that the radius of an ordinary liquid cluster in vapor scales as $N^{1/3}$ rather than staying finite.

5.2. Simulation results

We simulated the SDG model for $\eta = 0.03$ so as to validate our expectation that the coexisting fluid phases for not too large temperatures are, for δ sufficiently smaller than σ, a very diluted vapor and an extremely dense liquid. This would reinforce our argument that the extensive-to-nonextensive crossover line of the DG model can be interpreted as the ascending branch of the spinodal line of a transition between two fluids of highly different densities.

To reach this goal we employed a "deformed" SDG potential, where the power-law repulsion $\epsilon(\delta/r)^{24}$, rather than a hard core, is added to the DG potential (we call SDG also this version of the potential). Replacing the hard core with an inverse-power law will accelerate the attainment of equilibrium in Gibbs-ensemble simulations, without substantially altering the

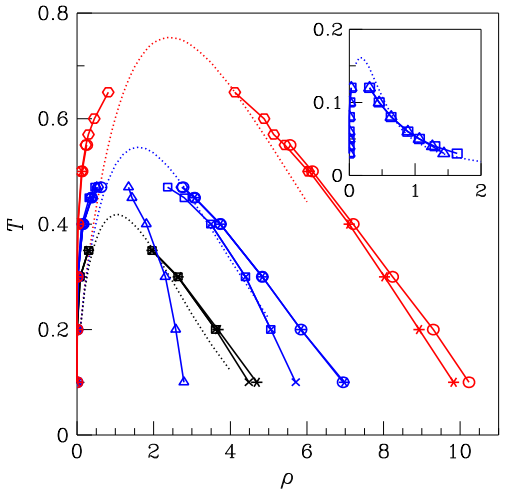

Fig. 10. SDG model for $\eta = 0.03$. Liquid–vapor coexistence lines derived from GEMC simulations carried out for three different δ values: from top to bottom, $\delta = 0.45$ (red), 0.5 (blue), 0.55 (black). Results for various sample sizes are shown: 864 + 864 (triangles), 2048 + 2048 (squares), 4000 + 108 (crosses), 4000 + 4000 (hexagons), 8192 + 128 (asterisks), and 16 000 + 128 (dots). Data points are joined by straight-line segments to guide the eye. For each δ, the BL of the HNC theory is also reported as a dotted line. Inset: Liquid–vapor coexistence for $\eta = 0.0265$ and $\delta = 0.5$. (For interpretation of the references to color in this figure legend, the reader is referred to the web version of this article.)

location of the coexistence line with respect to the hard-core case. In order to reduce the computational effort we cut off the SDG potential at a distance of 6σ and also shifted it vertically so as not to have to bother with long-range corrections to the energy and pressure. However, a long cutoff distance may affect the estimate of coexistence, which happens when the box length becomes smaller than twice the cutoff (*i.e.*, when the sample size is too small or the liquid density too high). To cope with this problem we collected data for a few increasing sample sizes until convergence is reached. In practice, with a maximum size of about 16 000, the lowest δ value which we could manage was 0.45, which is small enough to serve our purpose.

We show our results in Fig. 10. Here the data refer to three values of δ, namely 0.45, 0.5, and 0.55. As δ is reduced, the binodal line extends to higher densities and temperatures, as it was expected from the HNC theory. Moreover, at low temperature the vapor density is vanishingly small, whereas the liquid is very crowded, meaning that the coexistence pressure is nearly zero. Hence, a simpler method to draw the *liquid* branch of the binodal line would be to run simulations of the liquid at zero pressure. While 8000 particles were sufficient to reach size convergence of the data for $\delta = 0.55$, 16 000 particles were just enough for $\delta = 0.45$, and even more particles would be needed for still smaller δ. In the inset of Fig. 10 we reported data for $\eta = 0.0265$ and $\delta = 0.5$. Here finite-size effects are less important (2000 particles were sufficient to get convergence, except possibly for the lowest temperatures). In spite of the fact that the SDG potential is unbounded, the HNC theory turns out to be overall very accurate, especially at low temperature where the BL falls inside the binodal line as expected.

As far as the solid phase is concerned, we expect it to become thermodynamically stable only for densities higher than about δ^{-3}. To check this prediction we considered the $\delta = 0.5$ case. Giving up any pretension to compute the exact melting line, a goal which would unavoidably require a huge sample size, we just limited to a rough (rounded-down) estimate of the melting density obtained by isothermally expanding a face-centered-cubic (fcc) solid until the point where it spontaneously melts. Fig. 11 reports the outcome of this calculation for two system sizes, 864 and 4000 (the simulation was always started from a fcc crystal of density $\rho = 10$). As is clear from the picture, the purported melting line is weakly dependent on the system size and well separated from the descending branch of the liquid–vapor binodal line, meaning that the liquid phase is stable down to at least $T = 0.3$.

An independent estimate of the liquid stability boundary came from the so-called zero-RMPE criterion [34] (where RMPE stands for *residual multi-particle entropy*). This is a one-phase freezing criterion based on an expansion of the system excess entropy per particle $s^{\rm exc}$ in spatial correlations between groups of more than two particles [35–37]. In short, when the RMPE (which is defined as $s^{\rm exc} - s_2$, where s_2 is the pair entropy per particle) vanishes, the multi-particle contribution to entropy is bound to explode, signaling that solidification is near. As a matter of fact, the zero-RMPE density ($\rho_{\rm RMPE}$) is an excellent estimate of the freezing density for the Lennard-Jones system [38], as confirmed by a further calculation made for $T = 1.40$ and $N = 1372$ with the data of Ref. [31] (we found $\rho_{\rm RMPE} = 1.026$, to be compared with a freezing density of 0.987 and a melting density of 1.060). We computed $\rho_{\rm RMPE}$ for various temperatures, for $\delta = 0.5$ and $N = 4000$ (see Fig. 11), finding values that pretty well compare with the threshold of (mechanical) stability of the crystal. The agreement is good even at low temperature, where the behavior of the SDG model would depart more from hard-sphere like.

Summing up, for $\eta = 0.03$ numerical simulation confirms the picture already emerged from the HNC theory. When δ is progressively reduced to zero, the liquid–vapor region widens unboundedly while the melting line is pushed to infinity.

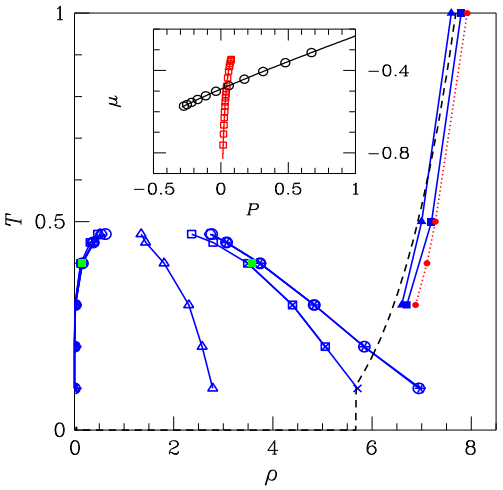

Fig. 11. SDG model for $\eta = 0.03$ and $\delta = 0.5$. The GEMC data for liquid–vapor coexistence are the same as shown in Fig. 10. The small green squares are the coexistence densities for $T = 0.4$ obtained for a system of 4000 particles by thermodynamic integration in the *NVT* ensemble: $\rho_v = 0.157$ and $\rho_l = 3.584$. On the high-density side of the picture, blue points mark the spontaneous melting of a fcc solid under isothermal expansion ($N = 864$, triangles; $N = 4000$, squares). For the same temperatures, the zero-RMPE melting threshold is marked by a red dot. The black dashed line is the melting line as predicted for the fcc crystal by the criterion introduced in Ref. [33] (in this case, a zero melting temperature denotes a mechanically unstable crystal). Inset: details of the crossing of vapor (red squares) and liquid (black dots) chemical potentials for $T = 0.4$ and $N = 4000$, occurring for $P = 0.0426$ and $\mu = -0.4788$. (For interpretation of the references to color in this figure legend, the reader is referred to the web version of this article.)

6. Conclusions

A colloid can be destabilized by suitably tuning its composition (*e.g.*, by adding salt or other depletant to the dispersion). Of a similar kind would be the phenomenon of protein aggregation underlying many forms of age-related brain diseases in man. While in colloids the tendency to aggregation eventually finds a stop in the existence of the particle core, which prevents particles from piling up one over the other, in some polymers (for instance, dendrimers) the centers of mass of two coils may even coincide. For such dispersions, aggregation would virtually proceed until all polymers occupy a small region of space. Indeed, a bounded potential which is sufficiently attractive at large distances belongs to the category, originally identified by Ruelle, of *catastrophic potentials*, *i.e.*, interactions that do not have a standard thermodynamics since the thermal averages are dominated by relatively few particle configurations (absorbing states) of exceedingly large density. As a result, these fluids decay to a non-extensive blob or cluster, which is also the attractor of the system dynamics. In practice, when the density of the aggregate overcomes a certain threshold, a description of inter-polymer forces in terms of a strictly pairwise potential ceases to be valid.

In the attempt to describe the onset of aggregation in purely schematic terms, we considered a specific model of bounded interaction, the DG potential. When the strength η of the interparticle attraction exceeds a threshold value η_c, the system becomes catastrophic. Approaching η_c from the stable side, we observed an anomalous widening of the liquid–vapor coexistence region, and the density of the saturated liquid grows without bounds near $T = 0$. In the unstable regime, we identified a line in the ρ–T plane separating a strongly-unstable region, where the system collapses to a spherical cluster very quickly, from a weakly-unstable (or metastable) region, where collapse is much delayed in time and the system is, to all practical purposes, stable.

To better clarify the nature of the metastable-to-unstable crossover we computed the characteristic time for collapse, finding that the range of densities where it grows substantially is indeed rather narrow. As the system size increases, the separatrix between the two regimes approaches a limiting position which well agrees with the boundary line (BL) (also dubbed *pseudospinodal line*) of the HNC theory. Even though these conclusions were obtained for a specific model of ultrasoft particles, we anticipate that they are more generally valid and applicable to other bounded potentials whose stability threshold is independently known [39].

The existence of two different behaviors in the unstable DG model finds a rationale in the shape of the HNC BL in the SDG model, obtained by augmenting the DG potential with a hard core of diameter δ. While the boundary lines of the two models are indiscernible up to a certain density, they increasingly depart from each other for higher densities, where a distinguished fluid–fluid transition appears in the SDG model. As δ is reduced, the overlap between the boundary lines of the two models extends to higher and higher densities. Hence, the collapse phenomenon observed in the DG model would not be much dissimilar from the *spinodal decomposition*, occurring in the SDG model for small δ, between two fluids of vastly different densities. A visible sign of spinodal behavior is the simultaneous development, when collapse first occurs, of many clusters which will merge together only at a later time. The phase behavior of the SDG model provides a clue to understand the coagulation of a colloid. When the strength of the large-distance (effective) attraction between the molecules

is progressively increased (e.g., by dissolving more salt in the dispersion), the system state will eventually be swallowed inside the expanding liquid–vapor region and a high-density condensate is formed, right as occurs for a SDG fluid.

References

[1] C.N. Likos, M. Schmidt, H. Löwen, M. Ballauff, D. Pötschke, P. Lindner, Macromolecules 34 (2001) 2914.
[2] A.A. Louis, P.G. Bolhuis, J.-P. Hansen, E.J. Meijer, Phys. Rev. Lett. 85 (2000) 2522.
[3] C.N. Likos, Soft Matter 2 (2006) 478.
[4] D. Ruelle, Statistical Mechanics: Rigorous Results, Imperial College Press, London, 1999.
[5] M.E. Fisher, D. Ruelle, J. Math. Phys. 7 (1966) 260.
[6] See, e.g. W. Pulawski, U. Ghoshdastider, V. Andrisano, S. Filipek, Appl. Biochem. Biotechnol. 166 (2012) 1626.
[7] S. Prestipino, C. Speranza, G. Malescio, P.V. Giaquinta, J. Chem. Phys. 140 (2014) 084906.
[8] C. Speranza, S. Prestipino, G. Malescio, P.V. Giaquinta, Phys. Rev. E 90 (2014) 012305.
[9] G. Malescio, S. Prestipino, Phys. Rev. E 92 (2015) 050301(R).
[10] F.H. Stillinger, J. Chem. Phys. 65 (1976) 3968.
[11] F.H. Stillinger, D.K. Stillinger, Physica A 244 (1997) 358.
[12] A. Lang, C.N. Likos, M. Watzlawek, H. Löwen, J. Phys.: Condens. Matter 12 (2000) 5087.
[13] S. Prestipino, F. Saija, P.V. Giaquinta, Phys. Rev. E 71 (2005) 050102(R).
[14] D.M. Heyes, G. Rickayzen, J. Phys.: Condens. Matter 19 (2007) 416101.
[15] R. Fantoni, A. Malijevský, A. Santos, A. Giacometti, Europhys. Lett. 93 (2011) 26002.
[16] R. Fantoni, A. Malijevský, A. Santos, A. Giacometti, Mol. Phys. 109 (2011) 2723.
[17] A.Z. Panagiotopoulos, Mol. Phys. 61 (1987) 813.
[18] D. Frenkel, B. Smit, Understanding Molecular Simulation, second ed., Academic, 2002.
[19] See, e.g. J.-P. Hansen, I.R. McDonald, Theory of Simple Liquids, fourth ed., Academic, 2013.
[20] F.J. Rogers, D.A. Young, Phys. Rev. A 30 (1984) 999.
[21] L.L. Lee, J. Chem. Phys. 103 (1995) 9388.
[22] C.N. Likos, Phys. Rep. 348 (2001) 267.
[23] G. Malescio, Mol. Phys. 112 (2014) 1731.
[24] C.N. Likos, A. Lang, M. Watzlawek, H. Löwen, Phys. Rev. E 63 (2001) 031206.
[25] C.N. Likos, B.M. Mladek, D. Gottwald, G. Kahl, J. Chem. Phys. 126 (2007) 224502.
[26] S. Prestipino, J. Phys.: Condens. Matter 24 (2012) 035102.
[27] M. Bowker, Nature Mater. 1 (2002) 205.
[28] S.V. Buldyrev, G. Malescio, C.A. Angell, N. Giovambattista, S. Prestipino, F. Saija, H.E. Stanley, L. Xu, J. Phys.: Condens. Matter 21 (2009) 504106.
[29] G. Franzese, G. Malescio, A. Skibinsky, S.V. Buldyrev, H.E. Stanley, Nature 409 (2001) 692.
[30] L.G. MacDowell, V.K. Shen, J.R. Errington, J. Chem. Phys. 125 (2006) 034705.
[31] M.C. Abramo, C. Caccamo, D. Costa, P.V. Giaquinta, G. Malescio, G. Munaò, S. Prestipino, J. Chem. Phys. 142 (2015) 214502.
[32] S. Prestipino, C. Caccamo, D. Costa, G. Malescio, G. Munaò, Phys. Rev. E 92 (2015) 022141.
[33] S. Prestipino, F. Saija, G. Malescio, J. Chem. Phys. 133 (2010) 144504.
[34] P.V. Giaquinta, G. Giunta, Physica A 187 (1992) 145.
[35] R.E. Nettleton, M.S. Green, J. Chem. Phys. 29 (1958) 1365.
[36] S. Prestipino, P.V. Giaquinta, J. Stat. Phys. 96 (1999) 135. Erratum in: J. Stat. Phys. 98, 507 (2000).
[37] S. Prestipino, P.V. Giaquinta, J. Stat. Mech. Theory Exp. (2004) P09008.
[38] P.V. Giaquinta, G. Giunta, S. Prestipino, Phys. Rev. A 45 (1992) 6966(R).
[39] G. Malescio, S. Prestipino, manuscript in preparation.